The Deformation Physics of Nanocrystalline Metals: Experiments, Analysis, and Computations

Marc A. Meyers, Anuj Mishra, and David J. Benson

This article presents a review of the principal mechanisms responsible for the plastic deformation of nanocrystalline metals. As the concentration of grain boundaries increases, with a decrease in grain size there is a gradual shift in the relative importance of the deformation mechanisms away from the ones operating in the conventional polycrystalline domain. This is predicted by molecular dynamics simulations that indicate a preponderance of dislocation emission/annihilation at grain boundaries and grain-boundary sliding when grain sizes are in the range 20–50 nm. Experiments show, in general, a saturation in work hardening at low strains, which is indicative of a steady-state dislocation density. This saturation is accompanied by an increased tendency toward shear localization, which is supportive of dislocation generation and annihilation at grain boundaries. Dislocation analyses recently proposed corroborate the computational predictions and provide a rational foundation for understanding the mechanical response.

INTRODUCTION

Nanocrystalline materials have been the subject of widespread research in recent decades; since the landmark paper by Gleiter[1] in 1983, and his subsequent review of 1989,[2] thousands of papers have been published on the topic. Nanocrystalline materials are single- or multi-phase materials organized in units having dimensions in the nanometer range ($1 \times 10^{-9} - 200 \times 10^{-9}$ m). These units can be structured in one, two, or three dimensions. At the lower end of this spectrum are the amorphous materials (glasses). Nanocrystalline materials are characterized by an increased density of grain boundaries which may significantly alter their mechanical properties: elastic modulus, yield stress, ductility, thermal softening, toughness, fatigue and creep resistance, and strain-rate sensitivity. Of all the nanocrystalline configurations and materials, this article is restricted to equiaxed homogenous metals.

See the sidebar for experimental results.

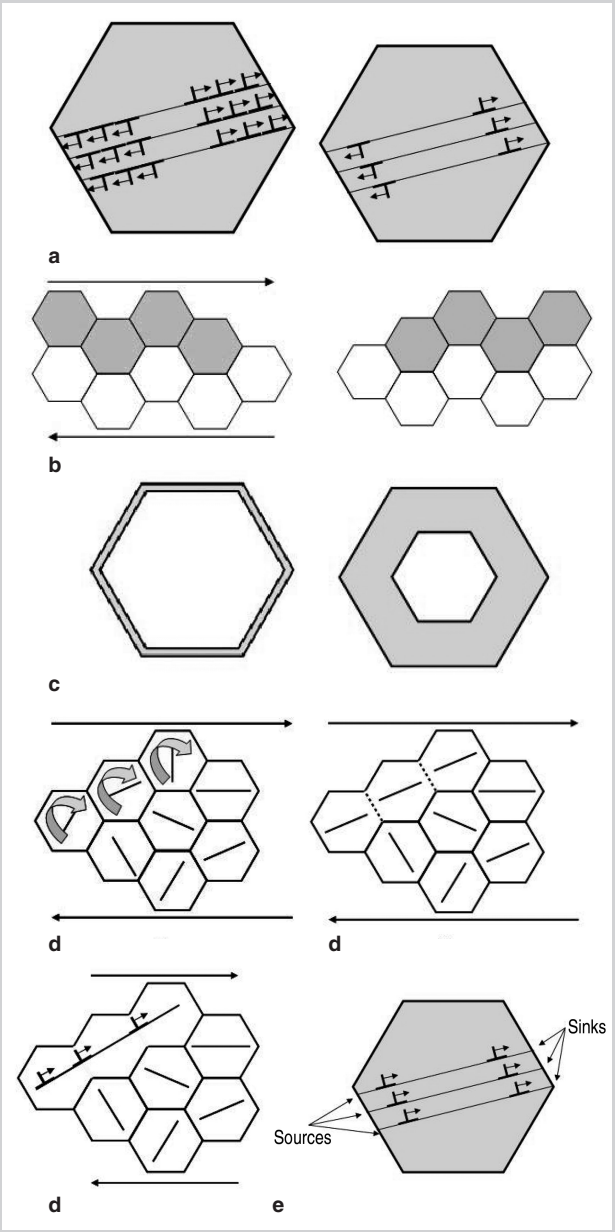

Figure 1. Sketches of different deformation mechanisms: (a) pile-up breakdown; (b) grain boundary sliding; (c) core and mantle; (d) grain coalescence; (e) sequential generation in grain boundary sources and annihilation in grain boundary sinks.

PHYSICAL MODELS FOR PLASTIC DEFORMATION

Dislocation Pile-Up at Grain Boundaries

The concept of pile-ups has been at the root of the traditional explanation for the H-P effect. Dislocations are assumed to be generated by Frank-Read sources and these are assumed to be in the center of the grain. As the grain size is reduced, the number of dislocations is eventually reduced to one and the stress amplification effect is lost. Figure 1a shows the individual dislocations (positive and negative) arrested at opposing grain boundaries. Thus, the pile-up mechanism breaks down. This mechanism was proposed by Pande et al.[20] and further developed by Armstrong and coworkers[21] for the loss in constancy in the H-P slope.

Grain-Boundary Sliding

In conventional polycrystalline metals, grain-boundary sliding by Coble creep only manifests itself at temperatures above 0.5 T_m. The negative H-P slope led Chokshi et al.[3] to propose that grain-boundary sliding plays a major role in nanocrystalline metal deformation at ambient temperature. This is a direct consequence of the equation for Coble creep, in which the strain rate, $d\varepsilon/dt = \dot{\varepsilon}$, is expressed in Equation 2. In this equation, D_{gb} is the grain-boundary diffusion coefficient, σ is the applied normal stress, G is the shear modulus, A_{Co} is a parameter, and d is the grain size. The strain rate is enabled at a stress level of 1,000 MPa (the approximate strength of nanocrystalline copper) and room temperature for copper with d = 20 nm is $d\varepsilon/dt = 10^{-3}\ s^{-1}$. This is in the realm of conventional plastic deformation. However, this simple grain-boundary sliding is not sufficient to accomplish the relative shear of grains, shown schematically in Figure 1b. There has to be plastic accommodation as was shown by Raj and Ashby[22] and Fu et al.[23] This introduces further difficulty into the process. Nevertheless, it seems that grain-boundary sliding becomes important for d<10 nm and could be responsible for the negative H-P slope in this domain. Thus, even as the experimental results by Chokshi et al.[3] are questionable and are probably

EXPERIMENTAL RESULTS

The difficulty of making realistic predictions of the strength of nanocrystalline metals based on experiments is illustrated by the results presented in Figure A, which represent a compilation of data from several sources for copper, probably the first or second most commonly studied metal. This plot is of the Hall-Petch type, albeit with the abscissa in nanometer units. Although for larger grain sizes the linearity is clear, for grain sizes of 100 nm or lower ($d^{-1/2} > 0.1\ nm^{-1/2}$) there is no clear trend. While some results show a decrease in the yield stress (negative Hall-Petch slope), some show an increase (positive Hall-Petch slope albeit of a lower magnitude), and others still a plateau. The negative Hall-Petch slope, which was observed and explained by Chokshi et al.,[3] is arguably one of the most contentious areas within the mechanical response of nanocrystalline metals. It should be emphasized that the processing route has significant effects. Voids, poorly bonded interfaces, interfacial impurities, and micro-/nano-cracks reduce the elastic modulus[4] and strength.[5] Indeed, the experimental results marked by full squares rotated by 45° in Figure A represent early tensile experiments by Nieman et al.[4] that are substantially lower than results obtained in compression (including hardness measurements, with the appropriate conversion $\sigma_y = H/3$). This is a clear indication of interface/void-initiated failure in tension. Weertman and coworkers[4–9] correctly and repeatedly attributed a great deal of the controversy in this field to the uncontrolled presence of these internal defects.

The strain-rate sensitivity of nanocrystalline metals, m, can provide a valuable fundamental deformation parameter: the activation volume V*, equal to bA*, where b is the Burgers vector and A* is the activation area for dislocation motion, which is the area swept by a dislocation overcoming obstacles in its course. They are related as shown in Equation 1, where T is the temperature, α is a parameter of the order of unity, and τ is the applied shear stress (note: all equations appear in the Equations table on page 45). The strain-rate sensitivity as a function of grain size for copper and nickel, two typical face-

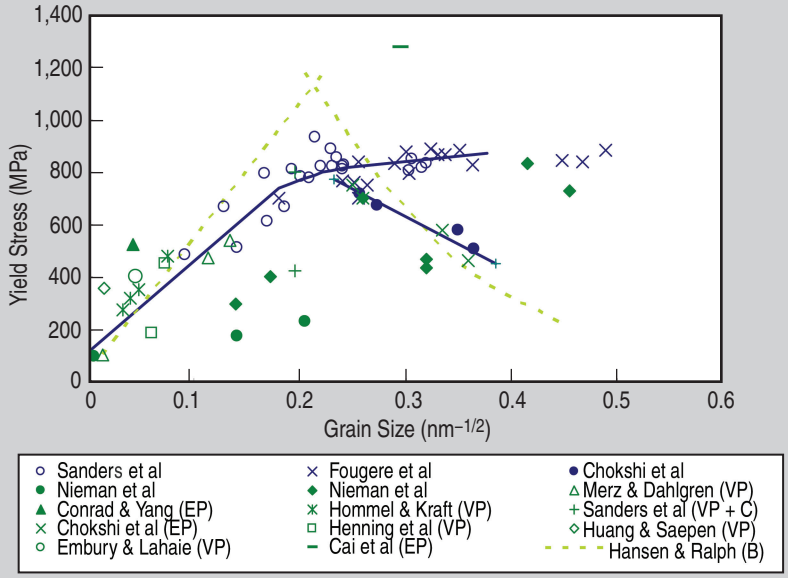

Figure A. The compiled yield stress versus grain size plot for copper from various sources ranging from coarse to nanograin size. The plots show different trend as the grain size falls below a critical size.

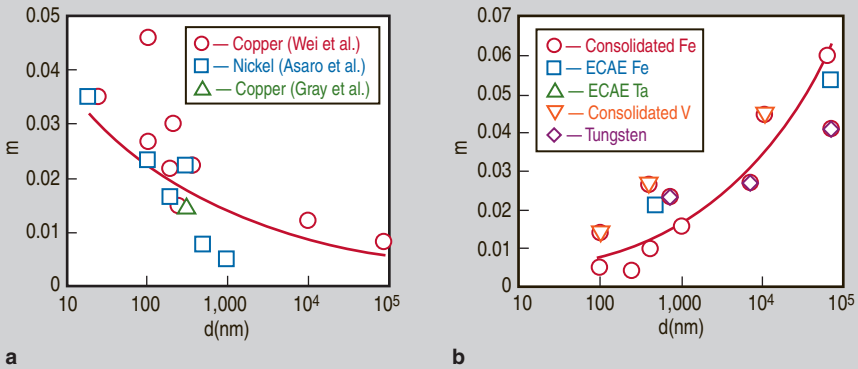

Figure B. The strain-rate sensitivity as a function of grain size for (a) fcc metals: Cu and Ni;[10–12] (b) bcc metals: Fe, Ta, V, and W.[13,14]

centered cubic (fcc) metals, is shown in Figure Ba.[10–12] There is a definite increase in m with a decrease in grain size. This corresponds to a decrease in V* from approximately (100–1,000)b^3 in the conventional polycrystalline range to ~10 b^3 in the nanocrystalline range.

For body-centered cubic (bcc) metals, the strain-rate sensitivity shows an opposite dependence on grain size. The results for Fe, Ta, V, and W are shown in Figure Bb.[13,14] Since the strength also increases with decreasing grain size (Hall-Petch relation), the product τm is approximately constant. Thus, V* is fairly independent of grain size and one does not expect a change in deformation mechanism in the nanocrystalline regime. The corresponding value of V* is of a few b^3.

The rate-controlling mechanism for conventional polycrystalline fcc metals is the cutting of dislocation forests by a moving dislocation. The activation area is equal to the spacing of forest dislocations multiplied by b and the activation volume is therefore equal to (100–1,000)b^3. In the nanocrystalline regime, the drastic decrease in V* to a few b^3 is suggestive of a change in the rate-controlling mechanism. Dislocation-boundary interactions or grain-boundary shear (mechanism chosen by Conrad[15]) are two possible mechanisms operating in the nanocrystalline regime.

For conventional polycrystalline bcc metals, the rate-controlling mechanism is the thermally activated motion of screw dislocations by the Seeger kink-pair lateral movement (analogous to a sidewinder snake). This is controlled by Peierls-Nabarro stresses which have an activation volume of a few b^3. The constancy in V* suggests a constancy in rate-controlling deformation mechanism. However, this cannot be assured, since other mechanisms with a small activation volume might become operative.

The compressive stress-strain curves for ultrafine-grained and nanocrystalline Cu, Fe, Ni, and Ti are shown in Figure C. It is clear that work hardening saturates at a very low plastic strain. This is a strong predictor for shear instability, since there are three key elements dictating shear localization: thermal softening $d\tau/dT$, which favors shear localization, and strain-rate sensitivity m and work hardening $d\tau/d\gamma$, which oppose shear localization. For nanocrystalline bcc metals, the three parameters drive shear band formation, and it is indeed prevalent. Figure D shows lines on a plastically deformed iron specimen showing that plastic deformation is concentrated in narrow bands.[16] For fcc metals the higher m opposes shear localization.

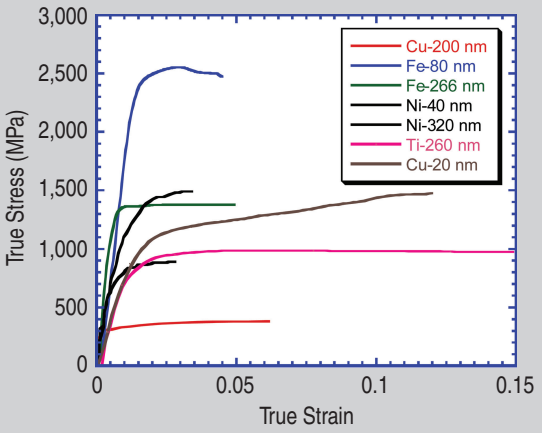

Figure C. The compressive stress-strain curves for ultrafine-grained and nanocrystalline Cu, Fe, Ni, and Ti (data from several sources).

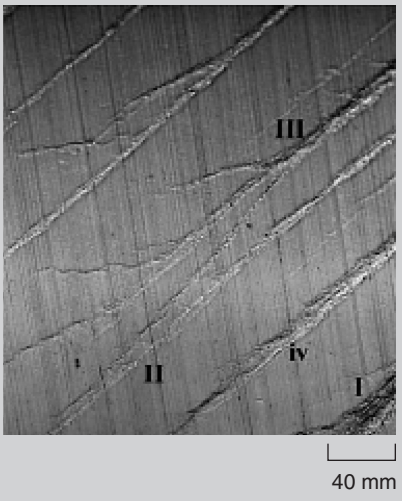

Figure D. The shear localization in ultrafine-grained (d = 268 nm) iron at a plastic strain equal to 0.078 (Figure 3[16]).

This paper is mainly concerned with fundamental deformation mechanisms in nanocrystalline metals. For a broad description of the mechanical properties of nanocrystalline and ultrafine-grained materials, including creep, fatigue, and ductility, the reader is referred to the overviews by Weertman and coworkers,[9,17] Kumar et al.,[18] and the one by the current authors.[19] This article will focus on the physical mechanisms proposed for this regime and on the elucidation of these mechanisms through computational approaches.

due to the use of a single sample repeatedly subjected to change in grain size by annealing, as correctly pointed out by Weertman,[8] there seems to be an effect of grain boundary sliding, either by Coble creep or by relaxation, as proposed by Fan et al.[24]

Core and Mantle Models

Li first recognized in 1963[25] that grain boundaries can serve as sources of dislocations. This approach was extended by Ashby[26] who proposed statistically stored and geometrically necessary dislocations, the latter required to accommodate the incompatibility stresses at the grain boundaries due to anisotropy (see Hirth[27]). Figure 1c shows a grain divided schematically into two regions; a central core and the grain-boundary region, called "mantle." The mechanical response of these two regions is different, with work hardening being more pronounced in the mantle. This is because the grain interiors are subjected to a more homogeneous state of stress, while in the mantle several factors contribute to the increased hardening: grain-boundary dislocation sources, change in orientation of plane of maximum shear, and elastic and plastic incompatibility. The ratio between the volumes of these two regions is dependent on grain size. There is ample experimental evidence for the development of a mantle in the conventional polycrystalline domain. The quantitative results by Zehetbauer et al.[28] are illustrative of this. Thus, one can develop expressions that predict the grain-size dependence of yield stress (e.g., Meyers and Ashworth[29] and Fu et al.)[23,30] As the grain size is reduced, the mantle becomes proportionally larger, as shown in the right side of Figure 1c.

Shear Band Formation

Shear-band formation is a major characteristic of the deformation of nanocrystalline metals and a direct consequence of the absence of work hardening, in many cases. This limited work hardening ability is a result of the lack of dislocation buildup with plastic deformation. The flow stress of a metal can be represented by the sum of the athermal (τ_G) and thermal (τ^*) components, as shown in Equation 3.

The athermal component represents the contribution of long-range barriers

(including the H-P component), the principal being the grain boundaries, whereas the thermal component represents point and line defect effects. τ^* may be expressed as shown in Equation 4, where ρ is the mobile dislocation density. If this density is constant, one has Equation 5. This shear-band formation can be aided by nanograin coalescence, which was observed by Wang et al.[31] Figure 1d shows how neighboring equiaxed nanograins can, upon rotating, create elongated grains that act as favored paths for plastic deformation because more extensive transit by dislocations is enabled. The major slip orientations and their rotation are marked in the grains by short segments in the centers of the grains.

Grain-Boundary Dislocation Sources and Sinks

As the grain size is reduced into the nanocrystalline range, dislocations can travel unimpeded throughout grains. Thus, dislocations emitted from one boundary can be annihilated in the opposite boundary. This is shown in Figure 1e. This was first observed in molecular dynamics (MD) and has been analytically described by Liao et al.[32,33] and Asaro et al.[34] using an energetic approach that equates the work to move the front dislocation segment to the energy of the screw segments left behind and deformation energy.

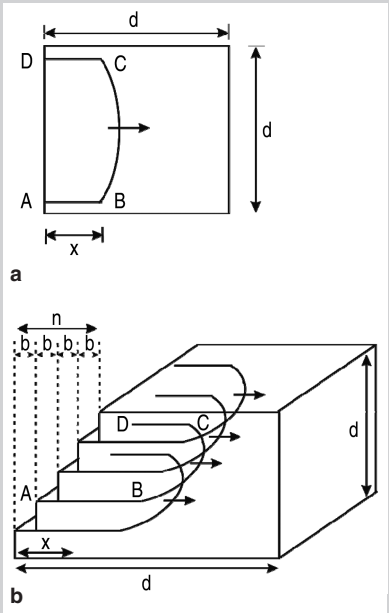

Figure 2. (a) A dislocation traveling through nanograin and leaving behind two segments AB and CD; (b) array of dislocations traveling through nanograin in parallel planes and creating a shear strain γ.

Figure 2a shows a dislocation emitted at a grain boundary AD and traveling partially through an idealized cubic grain. This dislocation, which is assumed to be of edge character, leaves behind two trailing screw dislocations: AB and DC. Figure 2b shows the tridimensional picture. An array of such dislocations was emitted from the left boundary and traveled an average distance x into the grain. The left side of the grain is deformed by a shear strain γ. The stress can be expressed, to a first approximation, as shown in Equation 6, where α is on the order of unity. For instance, for copper with a grain size of 50 nm, and assuming a = 0.5, b = 0.25 nm, one obtains τ = 242 MPa. For d = 20 nm, τ = 603 MPa. These values are on the same order of magnitude as the nanocrystalline strength.

The Role of Stacking Faults and Twinning

The surprising discovery of deformation twins in nanocrystalline aluminum by Chen et al.[35] has initiated a new cycle of study within this domain. Aluminum is a high stacking fault metal (γ =166 mJ/m^2) and previous attempts (low-temperature deformation, shock compression) had failed to yield mechanical twinning. Indeed, the current knowledge of mechanical twinning (e.g., Reference 36) predicts exactly the opposite: reduction of grain size makes twinning more difficult. This discovery, coupled with MD simulations showing profuse partial dislocation emission from grain boundaries, led to the analyses by Liao et al.[32,33] and Asaro et al.[34] that predict an increased separation of partials at the high stress level at which nanocrystalline fcc metals flow plastically. The expression obtained by Liao et al.[32] for the separation of partials, s_n, is given in Equation 7, where s is the partial separation in a monocrystal, γ is the stacking-fault energy, and υ is Poisson's ratio.

There seems to be clear indication that a threshold grain size exists at which perfect dislocations decompose into partials. Figure 3 shows the calculations by Zhu et al.[37] for aluminum. Three stresses are plotted against d : τ, the stress required to move a perfect dislocation; τ_p, the stress required to move partials; and τ_{twin}, the stress required to emit a twin from boundary. For the specific angle between the shear stress and dislocation line (=135°), the stress for partials becomes smaller than the stress for perfect dislocations for d < 17 nm. The twinning stress τ_{twin} is lower than both τ and τ_p. This is because it is easier to emit a second partial dislocation from a boundary adjacent and at a twin separation from the first partial. Partial emission is a necessary, but not a full, condition for twinning. For the twin to nucleate, the critical grain size needs to be much smaller than the grain size d = 17 nm. The critical grain size is actually determined by the stress below which a twin partial will need a lower stress than a trailing partial to move. The mechanical twins observed and modeled (by MD) in nanocrystalline metals are only a few atomic layers thick and therefore only require a few partial dislocations gliding on parallel planes.

COMPUTER SIMULATIONS

Two computer simulation approaches have been implemented: continuum modeling (finite-element method [FEM]) and MD. A third level of modeling, intermediate between these two, is dislocation dynamics. There is also a hybrid between MD and FEM, the quasicontinuum method. However, these methodologies have not been significantly applied to nanocrystalline materials.

Finite-Element Method

The finite-element method is a continuum modeling method, and therefore has no intrinsic length scale. Length scale effects must be introduced through the material models. Two approaches were used by Fu et al.[30] In the first approach, the grains are considered as consisting of two parts (this is a core and mantle approach): a grain boundary of finite thickness and the grain interior. The thickness of the grain boundary is assumed to be a non-linear function of the grain diameter. Figure 4 shows the grains, generated by Voronoi tessellation, divided into interiors and boundary regions. Two grain sizes are shown: 100 μm and 26 nm. The relative thickness of the grain-boundary region is quite different between the two. This results in differences in mechanical response.

In the second approach, called the gradient approach, a hardening model is introduced that is related to the dislocation density evolution. The evolution is assumed to be governed by the change in the orientation of the plane of maximum shear stress, which is measured by the gradient of the maximum shear stress angle. This gradient varies inside the grain, being maximum at grain junctions such as triple points. It is also linearly dependent on the grain size. Thus, a hardening function connected to the gradient will generate the grain size dependence of yield stress and work hardening. Figure 5 shows the distribution of magnitudes of the gradient of angle of maximum shear stress throughout a polycrystalline grain for two sizes: 1 μm and 26 nm. It can be seen that the gradient is larger for smaller d. This introduces a desirable and physically correct dimensional parameter into the FEM calculations.

Molecular Dynamics

The most important and significant results on the physical processes occurring during plastic deformation of nanocrystalline metals have been obtained by MD. The predictions of dislocation generation and annihilation at grain boundaries, of increased partial dislocation spacing, and of twinning are of special significance. A limitation of this technique is that the deformation times (10^{-9} s) are lower by many magnitudes than actual times at conventional strain rates (a few seconds to a few minutes). This technique is well suited for the study of nanocrystalline metals because of the limited number of atoms in each simulation. Although this number is continuously increasing (being a maximum of 10^8 in 2006), a volume of only approximately 1 μm^3 can be tested. For conventional polycrystals, such a volume would not be representative of the material but for a nanocrystalline metal with a grain size of 50 nm, the simulation incorporates 10^4 grains. Two groups have spearheaded the effort: van Swygenhoven and coworkers [e.g., References 38–40] and Yamakov, Wolf, and coworkers [e.g., References 41–44].

The MD simulation by Yamakov et al.[41] in Figure 6 shows aluminum with a grain size of 45 nm at a plastic strain of 0.12. The gray lines indicate regions where the stacking sequence has been altered. Several processes of plastic deformation involving grain boundaries are seen: heterogeneous nucleation of twin lamellae from the grain boundaries (e.g., τ_2 in grain 3); homogeneous nucleation of twin lamellae from the grain interior (e.g., τ_1 in grain 1); and growth of twin lamellae to form a new grain (grain A). The simulations predicted mechanical twinning in the deformation of a nanocrystalline aluminum-like material.

A depiction of the MD simulations by Froseth et al.[40] is shown in Figure 7. The applied stress is 1.6 GPa and the aluminum grain size is a 12 nm. In Figure 7a a partial dislocation has been emitted from the lower left hand corner of the grain. A second partial is emitted in 11b and the dark atoms represent the faulted region. The partials move through the grain (Figure 7c) and eventually are absorbed into the upper boundary. Froseth et al.[40] discuss the spacing of partials, noting that it is not uniform along the dislocation line.

More recently, this MD simulation effort has extended to Los Alamos National Laboratory[45] and Lawrence Livermore National Laboratory,[46–48] among other laboratories. It is fortuitous that MD simulations and laser shock experiments are so well matched. Indeed, the total deformation time in MD is on the order of 10^{-7}–10^{-9} s. This corresponds to the loading times in laser shock compression. Thus, results observations in shock compression can be directly compared with MD simulations. The MD image of a shock wave propagating through a nanocrystalline metal (d = 20 nm) is shown in Figure 8a.[47] The generation and emission of partial dislocations from grain boundaries is the principal mechanism. At the front, this process initiation is perfectly captured, whereas behind the front the partials have, for the most part, propagated through the entire grains. Perfect dislocations and nano-twins were also identified.[47] Transmission-electron microscopy (TEM) observations by Wang et al.[48] on nanocrystalline nickel subjected to compression of 20–70 GPa at a strain rate higher than 10^7 s^{-1} (isentropic compression) confirm the presence of these dislocations in nickel. Figure 8b shows a bright-field TEM of nickel subjected to a pressure of 40 GPa. The insert in Figure 8b is a dark-field image showing dislocation within the nanocrystalline grains. This high rate of loading and unloading freezes the deformation structure more effectively than quasistatic deformation and enables a more realistic observation of the dislocation processes. It can be seen that dislocations play an important role even at grain sizes in the 20–70 nm range.

Equations Table

$$V^*=bA^*=(\alpha kT)/(\tau m) \quad (1)$$

$$\dot{\varepsilon} = \frac{A_{Co} D_{gb} \sigma}{G d^3} \quad (2)$$

$$\tau=\tau_G+\tau^* \quad (3)$$

$$\tau^*=k\rho^{1/2} \quad (4)$$

$$d\tau/d\gamma=0 \quad (5)$$

$$\tau=\alpha Gb/d \quad (6)$$

$$\frac{S_n}{S} = \frac{\gamma}{\gamma = \frac{Gb^2(8+\upsilon)}{24\pi(1-\upsilon)d} \ln\frac{d}{b} - \tau b} \quad (7)$$

CONCLUSIONS

The intense research into plastic deformation of nanocrystalline metals being conducted globally is amazingly interactive with major efforts in the United States, China, Germany, and Russia. It has enabled rapid progress in the understanding of principal mechanisms operating in the ultrafine-grained/nanocrystalline regimes. This understanding has been gained from a combined three-pronged approach to the complex problem, involving experiments and characterization, analytical/physical modeling, and computations. Molecular dynamics computations are especially suited for nanocrystalline metals due to the limitation in the number of atoms (in the 10^6–10^8 range) and size (in the micrometer range). For the conventional polycrystal and ultrafine-grained regimes, FEM continuum approaches are more useful at present. Although all mechanisms described in this article may play a role under specific internal (grain size, composition, etc.) or external (temperature, strain rate, stress state) factors, a few seem dominant. The major mechanisms are, for the four grain domains which we consider:

1 μm > d > 100 nm (Ultrafine Grain Sizes)

A core-and-mantle model describes the response well. The models are based on dislocation generation at or adjacent to grain boundaries and on the formation of work-hardened grain boundary layers. Grain-boundary ledges with spacing of 10–100 nm provide an ample supply of starter dislocations that, upon emission into the grains, cross-slip and multiply, creating a work-hardened layer close to the grain boundaries. As the grain size is reduced, the ratio between volume fractions of the mantle and core increases, providing an increase in yield stress that can be expressed as a power equation d^{-n}, where n usually takes a value around 1/2 for grain sizes >1 μm and smaller than 1/2 in the region 1 μm d >100 nm.

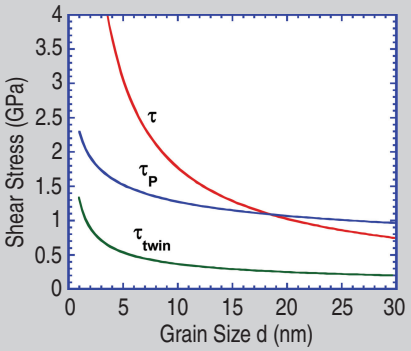

Figure 3. The stresses required for emission of perfect dislocation (τ), partial dislocation (τ_P), and twinning (τ_{twin}) as a function of grain size in the nanocrystalline regime for aluminum, assuming a value of a = 135° (adapted from Zhu et al.[37]).

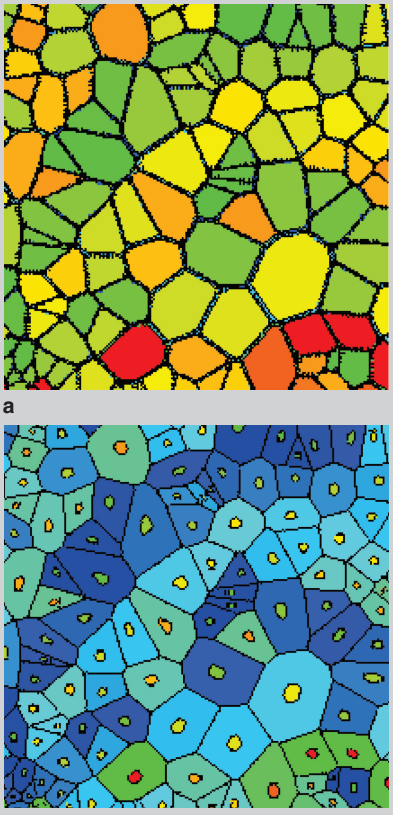

a

b

Figure 4. The simulated conventional polycrystalline and nanocrystalline metal used by Fu et al.[23,30] in FEM computations: (a) d = 100 μm, t = 3.33 μm; (b) d = 26 nm, t = 10.3 nm.

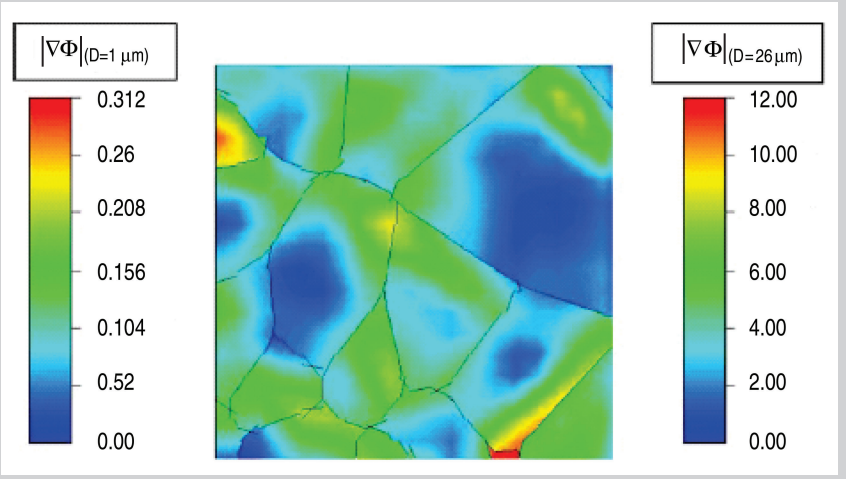

Figure 5. The distribution of magnitude of gradient of angle of maximum shear stress obtained by Fu et al.[30] Left-hand scale: d = 1 μm; right-hand scale: d = 26 nm.

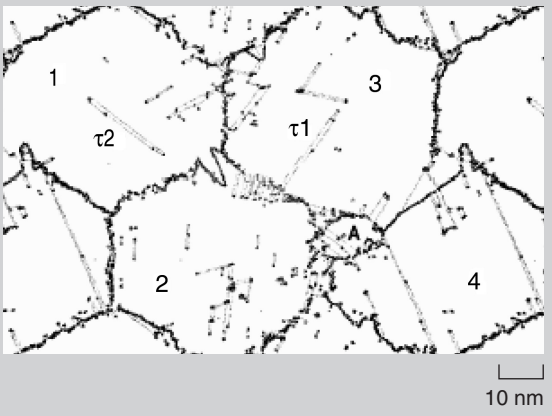

Figure 6. An MD simulation of nanocrystalline aluminum-like solid (d = 45 nm) having been subjected to plastic strain of 0.12; grey lines enclose regions with altered stacking sequence (from Yamakov et al.[41]).

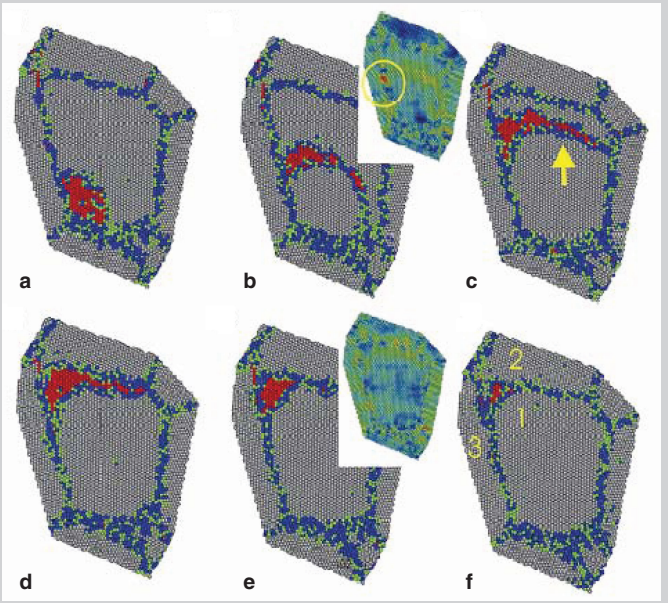

Figure 7. The MD computations obtained by van Swygenhoven and coworkers (Froseth et al.[40]) showing the formation of partial dislocation and its expansion throughout grain; notice trailing partial that recomposes perfect lattice (b,c). Red atoms are between partials.

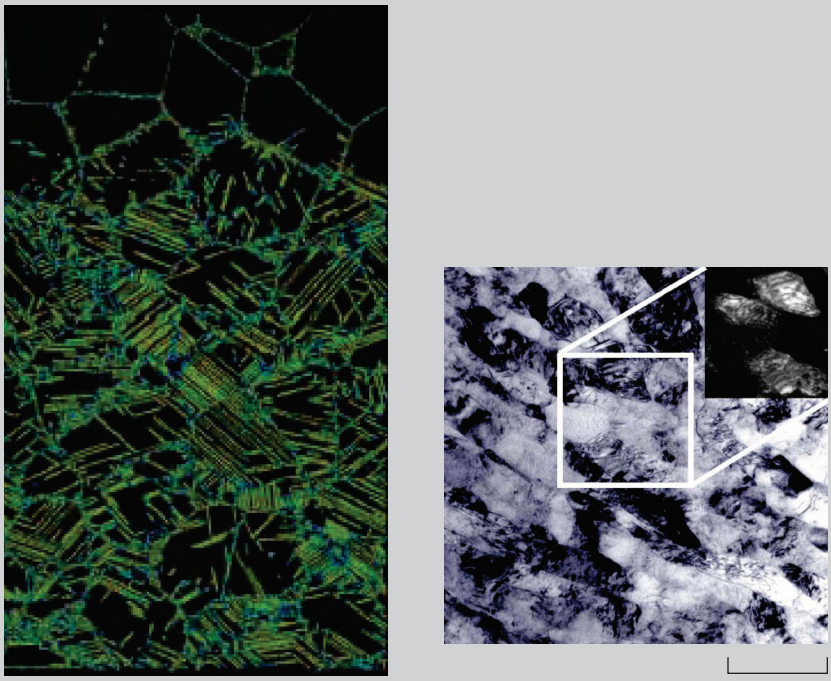

Figure 8. (a) A snapshot of a simulation for d = 20 nm and P = 47 GPa. The shock front, moving from bottom to top, produces a high density of partial dislocations (originating at grain boundaries), perfect dislocations (isolated inside grains) and nano-twins (courtesy of E. Bringa, Lawrence Livermore National Laboratory); (b) transmission-electron micrograph with dark field insert showing dislocation inside grains after nanocrystalline nickel was subjected to isentropic compression at 40 GPa and a strain rate >10^7 s^{-1} (from Wang et al.[48]).

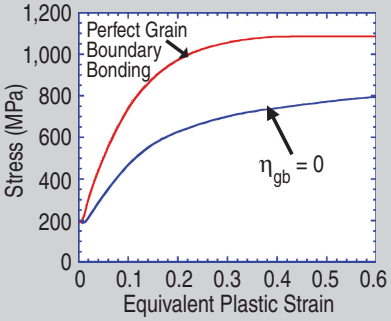

Figure 9. The computed (by FEM) mechanical response of nanocrystalline copper (d = 20 nm) assuming that grain boundaries have zero viscosity; the strength is still 2/3 of that of the equivalent material with perfect grain boundaries, proving that grain-boundary sliding can only be responsible for a fraction of plastic strain and that plastic deformation within grains has to be the dominant mechanism (from Fu et al.[23]).

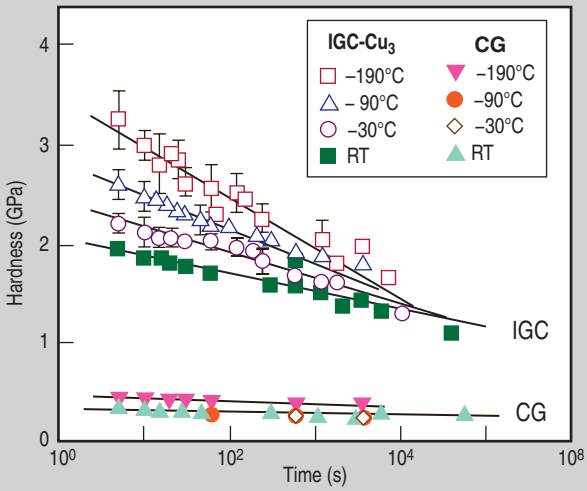

Figure 10. Hardness as a function of time for nanocrystalline(ICG-3) and conventionally grain sized (CG) copper (from Zhang et al.[49]).

100 nm >d >20 nm

In this region, the H-P slope continues to decrease with decreasing d. The grain-boundary ledges can no longer supply dislocations in this regime because their spacing (l < 30 b) becomes large with respect to the grain size. The dislocations emitted from grain boundaries have less and less chances of cross-slipping and multiplying in grains. They can travel through the grains relatively unimpeded and annihilate in the opposing boundary. This can be carried out without significant work hardening, since the density remains constant. This leads to shear localization.

20 nm >d >1 nm

In this regime, the grain-boundary effects dominate the deformation process. Grain-boundary sliding becomes important in this regime and has been identified by Conrad[9] and other researchers as the principal mechanism. However, grain-boundary sliding cannot occur by itself and needs associated plastic deformation. This is eloquently shown by the computer calculations of Fu et al.[30] and in Figure 9. The grain boundary shear strain was completely eliminated for one of the simulations, effectively creating a grain-boundary layer with zero viscosity. One would expect, at first, that the materials strength (in this case copper with a grain size of 20 nm) would drop to zero. This is not the case and the nanocrystalline copper retains approximately 2/3 of its original mechanical response.

1 nm >d >0 nm

Effectively, we move gradually from a nanocrystalline to an amorphous state, whose deformation is dominated by regions of intense shear.

There are, at this point, a number of unresolved issues in the field of nanocrystalline plastic deformation. The recent observations by Zhang, Eastman, and Weertman[49,50] of grain growth in nanocrystalline copper subjected to high stresses at temperatures as low as 83 K (–190°C) are indeed significant and point to boundary mobility effects that have heretofore not been considered. They monitored the hardness as a function of time up to 39 h and found that it decayed in the nanocrystalline domain, while

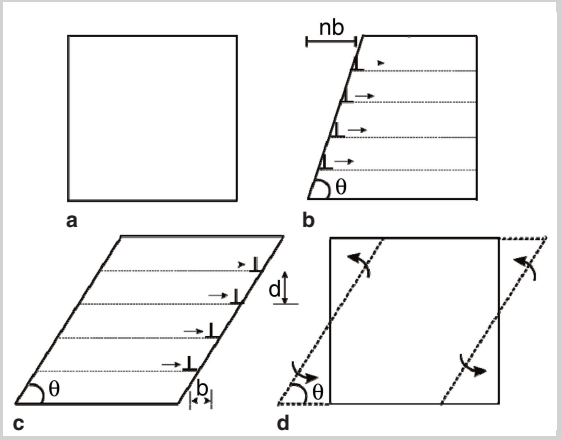

Figure 11.The sequential plastic deformation and grain-boundary rotations yielding steady state ultrafine equiaxed grains; (a) initial cubic grain configuration; (b) slip by dislocation emission from grain boundaries; (c) annihilation at opposite boundary; (d) deformed grain subjected to grain-boundary rotations leading to original grain configuration that will, in turn, be deformed by slip.

conventional polycrystalline copper did not exhibit this behavior. Figure 10 shows the relaxation curves. It is clear that the hardness is decreasing with time for the nanocrystalline copper while it is not for the conventional coarse-grained copper. This suggests a grain boundary mobility that is indeed intriguing. Diffusional mechanisms can hardly be invoked at these low temperatures.

A disclination model for grain boundaries incorporating dislocation emission was proposed by Hurtado et al.[51] and is especially relevant to the plastic deformation of nanocrystalline metals. This model enables the calculation of stresses required to emit dislocations from grain boundaries. The disclination dipole model is a better representation of large angle boundaries than a model comprised exclusively of dislocations because the latter ones can only represent some types (special) boundaries. The overlap of stresses of dislocations in random boundaries becomes too large with core interaction. Li[52] has also recently proposed an mechanism through which boundaries, comprised of dislocation arrays, migrate through the glide of dislocations.

One should consider that the nature of the boundary changes as dislocations are emitted. Figure 11 shows how an initially equiaxed grain is deformed by the imposed plastic deformation. If the equiaxed structure is to be retained, the boundaries need to rotate during or after plastic deformation (Figure 11d). These boundary mobility mechanisms, that are negligible in conventional polycrystalline metals, become important in nanocrystalline metals. This is an area where further research is warranted.

ACKNOWLEDGEMENTS

Support by the National Science Foundation under Grant CMS-0210173 (NIRT) is acknowledged. Discussions and collaborations with R.J. Asaro, B.K. Kad, M.E. Kassner, and G. Thomas are gratefully appreciated. Prof. J.C.M. Li, J. Weertman, and J.R. Weertman provided novel concepts which are briefly mentioned herein and will, hopefully, lead our future understanding of grain boundary mobility in nanocrystalline metals. M. Meyers would like to thank the generous hospitality of Dr. W. Proud and of the Cavendish Laboratory (University of Cambridge) Physics and Chemistry of Solids Group members.

References

1. H. Gleiter, *Proceedings of the 9th IVC-V (*Madrid, Spain, 1983). p. 397.
2. H. Gleiter, *Nanocrystalline Materials. Prog. Mater. Sci.,* 33 (1989), pp. 223–315.
3. A.H. Chokshi et al., *Scripta Mater.,* 23 (1989), pp. 1679–1684.
4. P.G. Sanders, J.A. Eastman, and J.R. Weertman, *Acta Mat.,* 45 (1997), p. 4019.
5. G.W. Nieman, J.R. Weertman, and R.W. Siegel, *J. Mater. Res.,* 6 (1991), p. 1012.
6. J. Youngdahl et al., *Scripta Mater.,* 37 (1997), p. 809.
7. S.R. Agnew et al., *Mat. Sci. Eng. A,* 285 (2000), p. 391.
8. J.R. Weertman, *Mat. Sci. Eng. A,* 166 (1993), p. 161.
9. J. Weertman, *Nanostructured Materials,* ed. C. Koch (Norwich, NY: Noyes Publications, 2002), pp. 393–417.
10. Q. Wei et al., *Mater. Sci. Eng. A,* 381 (2004), p. 71.
11. R.J. Asaro and S. Suresh, *Acta Mater.,* 53 (2005), p. 3369.
12. G.T. Gray et al., *Nanostruct. Mater.,* 9 (1997), pp. 477–480.
13. Q. Wei et al., *Acta Mater.,* 54 (2006), p. 77.
14. Q. Wei et al., *Acta Mater.,* 52 (2004), p. 1859.
15. H. Conrad, *Met. Mater. Trans. A,* 35A (2004), pp. 2681–2695.
16. D. Jia, K.T. Ramesh, and E. Ma, *Acta Mat.,* 51 (2003), p. 3495.
17. J.R. Weertman et al., *MRS Bulletin,* 24 (1999), p. 44.
18. K.S. Kumar, H.V. Swygenhoven, S. Suresh, *Acta Mater.,* 51 (2003), pp. 5743–5774.
19. M.A. Meyers, A. Mishra, and D.J. Benson, *Prog. Mat. Sci.,* 51 (2006), p. 061921.
20. C.S. Pande, R.A. Masumura, and R.W. Armstrong, *Nanostruct. Mater.,* 2 (1993), pp. 323–331.
21. R.W. Armstrong and G.D. Hughes, *Advanced Materials for the Twenty-First Century: The Julia Weertman Symposium,* ed. Y.W. Chung (Warrendale, PA: TMS, 1999), pp. 409–420.
22. R. Raj and M. Ashby, *J. Met. Trans.,* 2A (1971), p. 1113.
23. H.H. Fu, D.J. Benson, and M.A. Meyers, *Acta Mater.,* 49 (2001), pp. 2567–2582.
24. G.J. Fan et al., *Mat. Sci. Eng. A,* 400 (2005), p. 243.
25. J.C.M. Li, *Trans. Met. Soc.,* 227 (1963), p. 239.
26. M.F. Ashby, *Philos. Mag.,* 21 (1971), p. 399.
27. J.P. Hirth, *Met. Trans.,* 3 (1972), p. 3017.
28. M. Zehetbauer et al., *Acta Mat.,* 47 (1999), p. 1053.
29. M. Meyers and E. Ashworth, *Philos. Mag. A,* 46 (1982), p. 737.
30. H.H. Fu, D.J. Benson, and M.A. Meyers, *Acta Mater.,* 52 (2004), pp. 4413–4425.
31. Y.M. Wang, E. Ma, and M.W. Chen, *Appl. Phys. Lett.,* 80 (2002), pp. 2395–2397.
32. X.Z. Liao et al., *Appl. Phys. Lett.,* 84 (2004), p. 3564.
33. X.Z. Liao et al., *Appl. Phys. Lett.,* 83 (2003), p. 5062.
34. R.J. Asaro, P. Krysl, and B. Kad, *Philos. Mag.,* 83 (2003), p. 733.
35. M. Chen et al., *Science,* 300 (2003), p. 1275.
36. M.A. Meyers, O. Voehringer, and V. Lubarda, *Acta Mater.,* 49 (2001), p. 4025.
37. Y.T. Zhu et al., *Appl. Phys. Lett.,* 85 (2004), p. 5049.
38. H.V. Swygenhoven and A. Caro, *Nanostruct. Mater.,* 9 (1997), PP. 669–672.
39. H.V. Swygenhoven, A. Caro, and M. Spaczer, *Acta Mater.,* 47 (1999), pp. 3117–3126.
40. A.G. Frøseth, P.M. Derlet, and H. Van Swygenhoven, *Acta Mater.,* 52 (2004), p. 5870.
41. V. Yamakov et al., *Acta Mater.,* 49 (2001), p. 2713.
42. V. Yamakov et al., *Nature,* 1, (2002), p. 45.
43. V. Yamakov et al., *Acta Mater.,* 50 (2002), pp. 61–73.
44. A.J. Haslam et al., *Acta Mater.,* 52 (2004), pp. 1971–1987.
45. K. Kadau et al., *Metall. Mater. Trans.,* 35A (2004), p. 2719.
46. E.M. Bringa et al., *JOM,* 57 (9) (2005), p. 67.
47. E.M. Bringa et al., *Science,* 309 (2005), pp. 1838–1841.
48. Y.M. Wang et al., *Appl. Phys. Lett.,* 88 (2006), p. 061917.
49. K. Zhang, J.R. Weertman, and J.A. Eastman, *Appl. Phys. Lett.,* 85 (2004), p. 5197.
50. K. Zhang, J.R. Weertman, and J.A. Eastman, *Appl. Phys. Lett.,* 87 (2005), p. 061921.
51. J.A. Hurtado et al., *Mater. Sci. Eng. A,* 190 (1995), p. 1.
52. J.C.M. Li, "Mechanical Grain Growth," unpublished manuscript (2005).

Marc A. Meyers, Anuj Mishra, and David J. Benson are with the Materials Science and Engineering Program and Department of Mechanical and Aerospace Engineering at the University of California at San Diego.

For more information, contact Marc A. Meyers, University of California at San Diego, Materials Science and Engineering Program and Department of Mechanical and Aerospace Engineering, La Jolla, CA 92093-0411; (858) 534-4719; fax (858) 534-5698; e-mail mameyers@ucsd.edu.